Available online at www.sciencedirect.com
SCIENCE DIRECT®
Journal of Power Sources 140 (2005) 274–279
JOURNAL OF POWER SOURCES
www.elsevier.com/locate/jpowsour

Step response analysis of phosphoric acid fuel cell (PAFC) cathode through a transient model

Suman Roy Choudhury[a], Suhasini Roy Choudhury[a], J. Rangarajan[a], R. Rengaswamy[b,*]

[a] *Naval Materials Research Laboratory, Ambernath, Maharashtra, India*
[b] *Department of Chemical Engineering, Clarkson University, Potsdam, NY 13699-7505, USA*

Received 30 June 2004; accepted 30 July 2004
Available online 5 November 2004

Abstract

Transient state response analysis of phosphoric acid fuel cell (PAFC) cathode is important to understand various competitive processes like diffusion, reaction and product back diffusion occurring at various layers of the composite cathode. A two-dimensional unsteady state model for simulating PAFC cathode is developed as an extension of the previously developed steady-state model [S. Roy Choudhury, M.B. Deshmukh, R. Rengaswamy, A two-dimensional steady-state model for phosphoric acid fuel cells (PAFC), J. Power sources 112 (2002) 137–152]. The transient model is solved to study the impact of various parameters such as Tafel slope, diffusivity etc on the step response of the fuel cell. The effect of partial pressure variation in bulk gas for large sized PAFC cathode is also analysed. Trend analysis based on the model output is also experimentally verified using a small unit cell setup. The effect of various parameters on the settling time of the cathode, as revealed in this study, suggests possible development of a diagnostic tool employing such transient model.

Keywords: PAFC cathode; Steady-state model; Cathode diagnosis; Unsteady-state model

1. Introduction

Owing to diverse applications of phosphoric acid fuel cells (PAFCs), dynamic operation of a fuel cell stack is quite common. Such applications includes vehicular propulsion, hybrid backup systems, several military applications etc, where the load keeps fluctuating unlike steady on-site power generation systems.

A PAFC is composed of two porous gas diffusion electrodes, the anode and cathode. The gas after passing through porous substrate (diffusion layer) reaches the catalyst layer also termed as reaction layer. The catalyst layer is a porous layer, partly filled with electrolyte. The gas diffuses through the dry pores, dissolves in the electrolyte and then diffuses to the catalytic site. Oxygen reduction takes place on the site and the product water back diffuses through the diffusion layer to escape in the oxygen stream.

Unsteady state simulation of fuel cell is necessary to understand the system transient response under variable loads with various time constants. Apart from that, unsteady state simulation model is also important, to analyze the effect of disturbances of input variables even for a steady-state operation. A good representative transient state model can be used for diagnostics of a running stack, which is very important for high reliability applications such as hospital and military applications. The unsteady state model further finds its use in analyzing several control strategies to operate fuel cells, in the best possible way under diverse operating conditions.

2. Development of unsteady state model

The steady-state model for a PAFC (Fig. 1) presented in Choudhury et al. [1] is further extended to develop an unsteady state model. Bulk gas, i.e., oxygen flows in the Y-direction through the ribbed support over the left side of

* Corresponding author. Tel.: +1 315 268 4423; fax: +1 315 268 6654.
E-mail address: raghu@clarkson.edu (R. Rengaswamy).

0378-7753/$ – see front matter © 2004 Elsevier B.V. All rights reserved.
doi:10.1016/j.jpowsour.2004.07.035

Nomenclature

A^*	cross section area of an agglomerate in YZ plane [cm^2]
A_c	cross section area of each groove [cm^2]
a_a	effective area of catalyst site per unit volume of agglomerate [$cm^2\ cm^{-3}$]
a_c	groove cross section [sqcm]
b	normal Tafel slope [V per decade]
c_{os}	concentration of oxygen on surface of agglomerate [$gmol\ cm^{-3}$]
c_{1a}	concentration of oxygen inside agglomerate [$gmol\ cm^{-3}$]
$c_{H_3PO_4}$	phosphoric acid concentration in percent ortho phosphoric acid equivalent
D_{agg}	diffusivity inside agglomerate for oxygen [$cm^2\ s^{-1}$]
D'_{agg}	diffusivity inside liquid encapsulation on agglomerate for oxygen [$cm^2\ s^{-1}$]
D_d	diffusivity in diffusion layer for oxygen-water [$cm^2\ s^{-1}$]
D_r	diffusivity in reaction layer for oxygen-water [$cm^2\ s^{-1}$]
D_{hc}	hydraulic dia of each groove [cm]
E	open circuit potential [V]
E^0	standard open circuit potential [V]
$E1$	oxygen electrode (solid carbon phase) potential [V]
$E2$	local electrolyte (liquid) potential [V]
f	friction factor
F	Faraday constant [96,500 coulomb g^{-1} equivalent weight]
H	Henry's constant for oxygen solubility in phosphoric acid [$gmol\ cm^{-3}\ atm^{-1}$]
i_a	local current density [$A\ cm^{-2}$]
i_0	exchange current density for oxygen reduction on Pt [$A\ cm^{-2}$]
i_x	current in X-direction [A]
$j(x)$	flow of cation in X-direction [A]
$j(y)$	flow of cation in Y-direction [A]
k	reaction constant of oxygen reduction reaction
l_c	groove length [cm]
m_i	product of molar flux of ith species at gas electrode interphase in X-direction and width of the cell [$mol\ cm^{-1}\ s^{-1}$]
m_{i0}	inlet molar flow rate of ith species [$gmol\ s^{-1}$]
n	number of electrons taking part in the reaction
n_s	grooves per manifold
$N1$	number of agglomerate exposed per unit sqcm area in YZ plane
O_{rr}	oxygen reduction rate [$gmol\ s^{-1}\ cm^{-3}$]
P_T	total pressure (atm)
p_i	partial pressure of the ith species (atm)
p_{i0}	partial pressure of the ith species at inlet (atm)
R	universal gas constant [$atm\ cm^3\ gmol^{-1}\ K^{-1}$]
R_{agg}	average radius of an agglomerate [cm]
r	radial dimension inside an agglomerate originating at the center [cm]
T	system temperature in Kelvin scale
t	time [s]
U	oxygen reaction potential w.r.t. the reference [V]
W	width of the cell in Z-direction (cm)
$W(max)$	maximum electrical work available [W]
ΔE^0_{rev}	standard half cell potential w.r.t. hydrogen electrode [V]
α	activation coefficient
ϵ	capacitance per unit volume of reaction layer [$farad\ cm^{-3}$]
η	local overpotential [V]
η_0	overpotential at the bulk-electrolyte and electrode interphase [V]
κ_e	electrolyte conductivity [$mho\ cm^{-1}$]
κ'_e	electrolyte conductivity inside agglomerate core [$mho\ cm^{-1}$]
λ_d	porosity of diffusion layer
λ_r	porosity of reaction layer
ρ_a	agglomerate density inside reaction layer [$number\ cm^{-3}$]
Ψ	flow per manifold at system temperature and pressure [$cc\ s^{-1}$]

Subscripts for ith species

1	oxygen
2	water

the electrode. As the gas flows, part of the oxygen diffuses through the porous substrate of the electrode. The diffusion of oxygen is in X-direction.

Diffusion of oxygen and back diffusion of water vapor in the porous substrate for unsteady state can thus be defined by equation 1 which is as follows

$$\left(\frac{D_d}{RT}\right)\left(\frac{\partial^2 p_i}{\partial x^2}\right)+\left(\frac{D_d}{RT}\right)\left(\frac{\partial^2 p_i}{\partial y^2}\right) = \left(\frac{\lambda_d}{RT}\right)\left(\frac{\partial p_i}{\partial t}\right) \qquad [i=1,2] \tag{1}$$

Similarly, inside the reaction layer, mass transfer with reaction can be described by Eq. (2)

$$\left(\frac{D_r}{RT}\right)\left(\frac{\partial^2 p_i}{\partial x^2}\right)+\left(\frac{D_r}{RT}\right)\left(\frac{\partial^2 p_i}{\partial y^2}\right) = \Gamma+\left(\frac{\lambda_r}{RT}\right)\left(\frac{\partial p_i}{\partial t}\right) \tag{2}$$

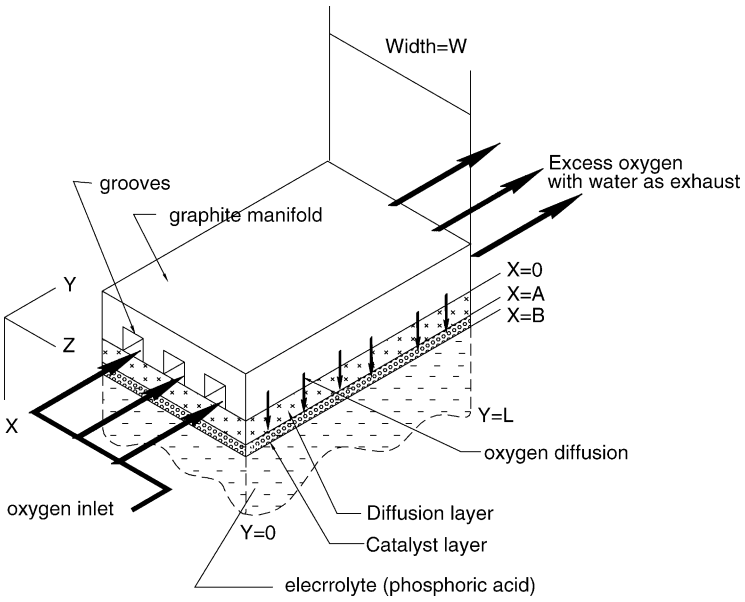

Fig. 1. View of PAFC cell.

where

$$\Gamma = 4\pi\rho_a D_{agg} R_{agg} c_{os}[\phi(R_{agg}) \coth \phi(R_{agg}) - 1] \quad (3)$$

$$\phi(R_{agg}) = \sqrt{\left(\frac{a_a k}{D_{agg}}\right)} \left[R_{agg} \exp\left(\frac{-2.3\eta}{2b}\right)\right] \quad (4)$$

and

$$c_{os} = Hp_1 \quad (5)$$

It is assumed that the agglomerates being very small in size will react very fast to the local surface gas partial pressure and hence the unsteady state contribution of the agglomerates are not considered.

Distribution of overpotential inside the catalyst layer can be modeled as done for the steady-state model, by considering ohmic law for the cation flow [2], in this case hydrogen ions, in the electrolyte filled zone. Thus, change of overpotential in X- and Y-directions can be related to the current flux as follows

$$\frac{\partial^2\eta}{\partial x^2} + \frac{\partial^2\eta}{\partial y^2} = \frac{(nF\Gamma)}{\kappa_e A^* N1} + a_a\epsilon\left(\frac{\partial\eta}{\partial t}\right) \quad (6)$$

The capacitance per unit volume of catalyst layer $a_a\epsilon$ arises primarily from the double layer near the active Pt sites.

3. Boundary conditions

Providing boundary conditions for solving the unsteady state simulation depends upon the mode of operation, starting conditions etc.

Following are two most common mode of operation:

Type-1: The system is running under steady state, and from that one or more operating parameters like gas flowrate, electrical load, humidity level is changed with respect to time.

Type-2: Inlet and outlet of the system is closed and heated up to the required temperature and then suddenly the valves were open to start the cell with operating parameters varied with respect to time.

Type-1 operation is of primary importance as it is the condition that is valid once the cell has started. Information regarding the initial values of the dependent variables over the region at time $t = 0$ is provided from the steady-state simulation of the steady state from which the changeover of operating parameters is considered.

Boundary conditions numbered 1–10 as mentioned in Choudhury et al. [1] for time > 0 is used as well. Depending upon the nature of variation of operating conditions with respect to time, the particular conditions are replaced with the time dependent profile of the same. For e.g., if the load is changed suddenly, then condition no. 7 [1] may be modified as follows:

$\eta = \eta_0$ at $t \leq 0$ and $\eta = \eta_1$ at $t > 0$ at $x = B \quad \forall y$

In case of change of inlet flowrate or concentration, the particular boundary conditions are modified accordingly.

3.1. Experimental setup for dynamic data acquisition

The experimental setup for validation of the unsteady state model is similar to that of the unit cell study as mentioned in Choudhury et al. [1]. A computerised data acquisition system is added to record the transient output of the cell. The

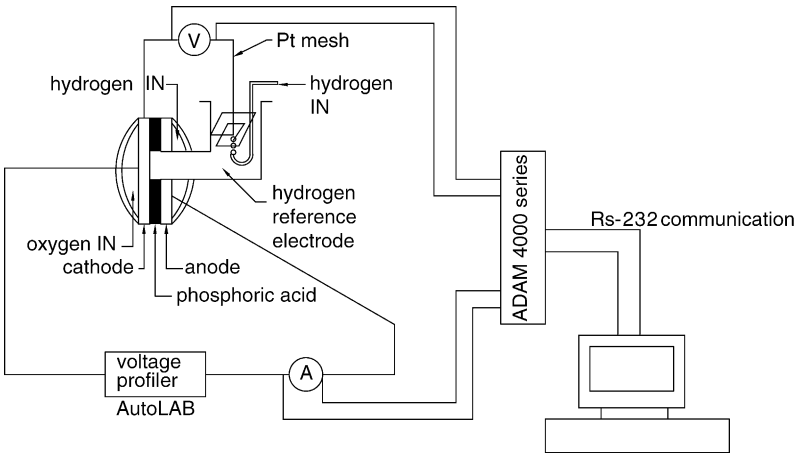

Fig. 2. Unit cell experimentation setup for transient response measurement.

compensator circuit is replaced with a high current electrochemical workstation (AutoLAB)which works as a variable load and any potential profile can be generated with this system. A secondary PC monitors the cell performance. Fig. 2 shows the complete experimental setup. A unit cell setup was used as the ionic transient potential is required to be measured to check the capacitance effect. The data acquisition card used is analog subsystem, FIFO, non-multiplexing type, from Advantech, USA. It has a maximum sampling speed of 100 sample per second per channel.

4. Analysis of the simulated results

The unsteady state model is solved using the software, Pdease2D that is used for solving the steady-state model [1]. The time dependent part is solved by marching forward method. After a small time increment, the partial pressure along the bulk gas flow interphase is updated as mentioned in the solution to the steady state model [1]. In this work, the effect of variations in the model parameters on step response of the electrode is tested. Values of the parameters assumed are provided in the Table 1, unless mentioned otherwise in the figures.

The simulated response is normalized by the final steady-state value. This is done in order to understand the response time better by making the ordinate scale same. We first report the results for the one-dimensional model. Fig. 3 depicts the simulated one-dimensional current response over a step jump from 0.1 V to 0.2 V overpotential at varying tafel slopes. The figure shows that as the tafel slope decreases, the peak increases, although the curve becomes more steeper, and the time required to attain steady-state value also decreases. Increase of the peak current with decreased tafel slope is expected, as sudden increase in overpotential along with the local high reactant concentration generates higher current. This effect also consumes the excess reactant faster and sets up the diffusion pattern early so that the settling time is decreased. Thus, the model result matches with the expected behavior.

Fig. 4 depicts the simulated step response for two values of reaction layer diffusivity. As the diffusion coefficient of the reaction layer increases, the normalized peak current increases along with the settling time. Due to enhanced diffusion properties, the steady-state current is higher. Thus, the normalized current which is a ratio between the transient current and the final steady-state current shows a smaller peak at the potential changeover time for the lower diffusivity case. Owing to better diffusion characteristics, the settling time is

Table 1
Values of parameters

Parameter name	Value	Remark
A^*	πR_{agg}^2 cm^2 of projection in YZ plane	Literature
a_a	3.5E04 cm^2 cm^{-3} of agglomerate	Experimental
b	60 mV per decade	Tuning
D_{agg}	1.0E−04 cm^2 s^{-1}	Literature
D_r	0.2E−03 cm^2 s^{-1}	Literature
Diffusion layer	400 μm thick	Experimental
E	0.92 V	Experimental
H	5.5E−08 gmol cm^{-3} atm^{-1}	Literature
i_0	1.0E−06 A cm^{-2}	Literature
n	4	Stoichiometry
$N1$	$0.5/\Pi R_{agg}^2$	Literature [2]
R_{agg}	1.0E−04 cm	SEM picture
Reaction layer	400 μm thick	Experimental
T	150 + 273 K	Experimental
W	10 cm	Experimental
κ_e	Function of phosphoric acid concentration	Model
ρ_a	$(3/4)[0.5/(\pi R_{agg}^3)]$	Literature
λ_d	0.5	Experimental
λ_r	0.5	Experimental
a_c	0.2 sqcm	Experimental
n_s	13 grooves per manifold (Type-A)	Experimental
D'_{agg}	D_{agg}/λ_r	Literature
κ'_e	0.25	Literature

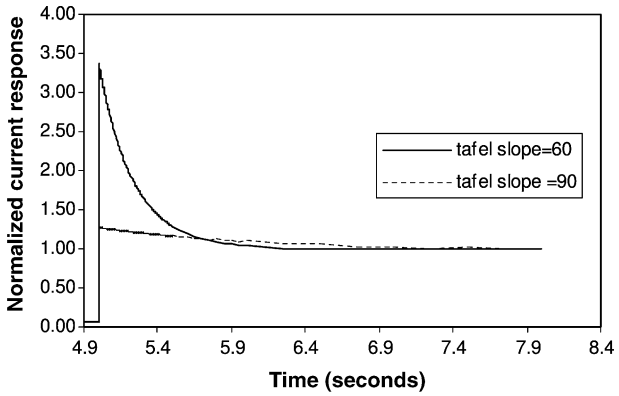

Fig. 3. Simulated step response at different tafel slope ($b = 60$ and 90 mV/decade) in one-dimensional mode.

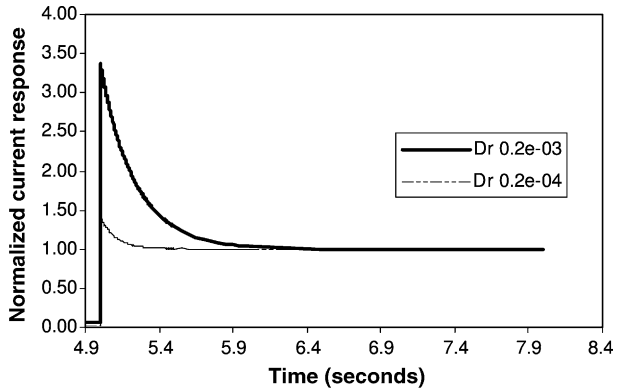

Fig. 4. Simulated step response at different diffusivity value in one-dimensional mode.

increased as better "supply" of reactant allows slow reduction of the current.

After checking the one-dimensional model, the two-dimensional model is simulated. Fig. 5 depicts the steady-state oxygen profile prior to the step change. Here, a simple "Type-A" groove, as mentioned in [1], which is composed

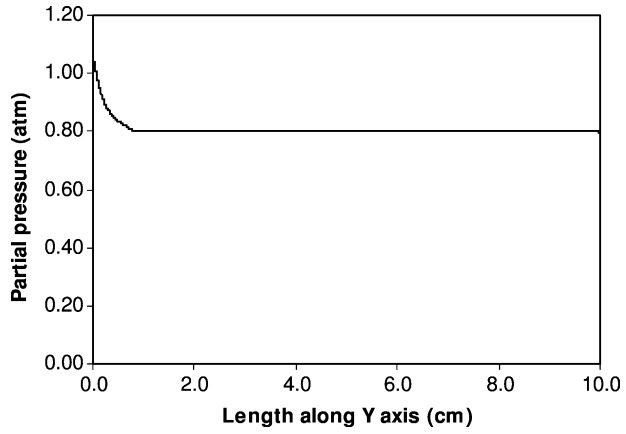

Fig. 5. Simulated oxygen profile prior to a step jump in two-dimensional mode.

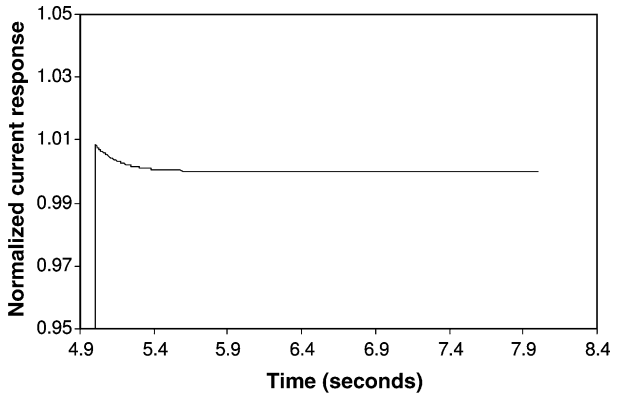

Fig. 6. Simulated step response in two-dimensional mode.

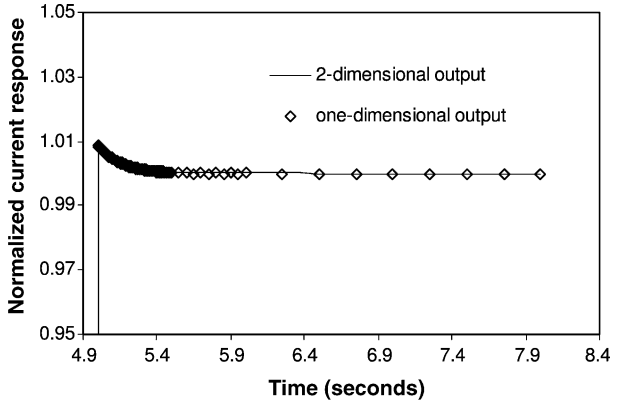

Fig. 7. Simulated one- and two-dimensional step response.

of all parallel channels is used. This groove has already been described in the steady-state model validation section of [1]. The flow rate used is $1\,l\,m^{-1}$ of oxygen flow per cell. Fig. 6 depicts the step response of the model. This response if plotted with the same parameters but using the one-dimensional model shows that the behavior is virtually the same as shown in the Fig. 7. This feature could be quite helpful for diagnostic purposes. For example, if the DC polarization performance of a large format cell decreases, and there is also a change in settling time, it implies that the possible reason could be some problem in the electrode rather than partial blocking or low gas flow rate.

5. Experimental results

5.1. Varying reaction layer diffusivity

Reaction layer diffusion is highly important as the PAFC cathode performance depends largely on the supply of reactants to the active sites and back diffusion of water. As the cathode ages, owing to mild carbon corrosion at the teflon–carbon interphase, more active area is wetted by the phosphoric acid. This increases the total active area inside the reaction layer. However, as the wetting increases, the dry pores

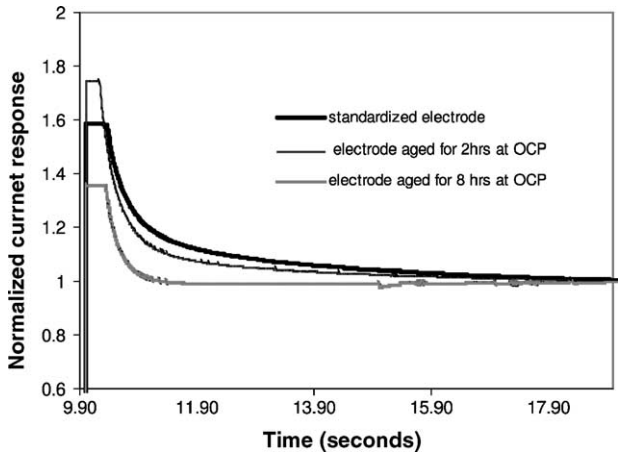

Fig. 8. Experimental step response of unit cell cathode of 0.1 V to 0.2 V overpotential change.

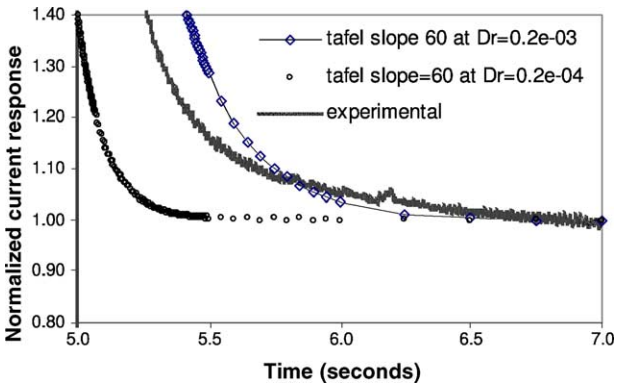

Fig. 9. Experimental step response with simulated data.

inside the reaction layer decreases. This results in lowering of effective gas diffusivity. Initially, as the cathode ages, the performance increases although the diffusivity is lowered. However, as the wetting passes a certain limit, due to severe drop in diffusivity, the overall cathode performance start decreasing.

The effect of cathode reaction layer diffusivity, on settling time, is studied using the unit cell setup as described before. The cathode is prepared as mentioned in [1]. The cell after soaking in 88% phosphoric acid for 24 h at a temperature of 150 °C, is assembled and operated for 4 h at a current density of 200 mA cm^{-2}. All the readings are taken after this initial conditioning of the cathode to stabilize the system. In order to age the cathode, so that the diffusivity of the electrode reduces, a rapid aging method is implemented. The cell is kept at open circuit mode for several hours after the initial conditioning. The step response analysis is done after different hours of aging to understand the trend.

Fig. 8 depicts the result of the step response. It can be seen that as the cathode ages, the settling time decreases. This results matches quite well with the simulation result as depicted in Fig. 4.

5.2. Matching of electrode response with simulated data

The normalized experimental result of the unit cell as mentioned in the Section 3.1 is plotted along with various other simulated data in the Fig. 9. It can be seen that the result is matching when the tafel slope is 60 mV per decade, which is that of the polished Pt surface, with the other parameters remaining same as in the Table 1. However, the previously tuned data for steady-state analysis [1] shows a tafel slope of around 120 mV per decade. This discrepancy could be analyzed as follows. The tafel slope of a rough catalyst surface as expected in the PAFC cathode catalyst is higher than the polished Pt surface due to near surface convection which is not modeled. Only bulk diffusion inside the agglomerate is considered while developing the agglomerate model. For the short transient period, the response thus matches with the real tafel slope value.

6. Conclusion

The models developed are studied for step response. It is observed that the settling time depends on several electrode related parameters such as diffusivity, tafel slope etc. However, the settling time remains the same for concentration gradient along the bulk flow, which is external to the electrode. This aspect may be valuable for diagnostic purposes. For example, same settling time of a normal cell and a faulty cell might indicate an external reactant blockage in the gas flow grooves, and the basic cell is not affected. As a cell ages, the wettability of the electrode increases, thus increasing the active area of the electrode, but decreasing the reaction layer diffusivity. The extent of electrode wetting in a newly assembled cell can be ascertained though the step response, as suggested by the simulation in Fig. 4.

References

[1] S. Roy Choudhury, M.B. Deshmukh, R. Rengaswamy, A two-dimensional steady-state model for phosphoric acid fuel cells (PAFC), J. Power Sources 112 (2002) 137–152.
[2] H. Celikar, M.A. Al-saleh, S. Gultekin, A.S. Al-zakri, A mathematical model for performance of raney nickel metal gas diffusion electrodes, J. Electrochem. Soc. 138 (6) (1991) 1671–1681.